Oxidized Diamond as a Simultaneous Production Medium of Carbon Nanomaterials and Hydrogen for Fuel Cell

Kiyoharu Nakagawa,[†,‡] Masa-aki Yamagishi,[‡] Hiro-aki Nishimoto,[‡]
Na-oki Ikenaga,[‡] Toshimitsu Suzuki,[‡] Tetsuhiko Kobayashi,[§]
Mikka Nishitani-Gamo,[||] and Toshihiro Ando*[,⊥]

National Institute for Materials Science (NIMS), 1-1, Namiki, Tsukuba, Ibaraki, 305-0044, Japan, Department of Chemical Engineering, Kansai University, Suita, Osaka 564-8680, Japan, Special Division for Green Life Technology, National Institute of Advanced Industrial Science and Technology (AIST), Ikeda, Osaka 563-8577, Japan, Institute of Applied Physics and Center for Tsukuba Advanced Research Alliance (TARA), University of Tsukuba, Tsukuba, Ibaraki 305-8577, Japan, and Core Research for Evolutional Science and Technology (CREST) of Japan Science and Technology Corporation (JST) and National Institute for Materials Science (NIMS), 1-1, Namiki, Tsukuba, Ibaraki 305-0044, Japan

Received November 21, 2002. Revised Manuscript Received July 15, 2003

High yields of hydrogen and carbon nanomaterials can be obtained by the decomposition of methane using oxidized diamond-supported Ni and Pd catalysts at 873 K. This is the first report to show that oxidized diamond can serve as an active support material. The simultaneous synthesis of carbon nanomaterials and hydrogen is especially interesting. Oxidized diamond is proposed as a novel catalytic means for the synthesis of hydrogen and carbon nanomaterials, and it is suggested that oxidized diamond may catalyze unique reactions of importance in nanomaterial synthesis.

Introduction

The production and utilization of nanocarbon materials such as fullerene and carbon nanotubes have attracted much attention recently.[1] The surface chemistry of diamond has recently been investigated, and several functional groups have been introduced on the diamond surface.[2] The surface of diamond is easily oxidized by reagents such as HNO_3, HClO, H_2O_2 etc., and also oxidized with O_2 at elevated temperatures to form C−O−C ether-type structures and C═O carbonyl-type structures.[3] Recently a great deal of attention has been focused on the unique characteristics, especially the surface properties, of diamond and oxidized diamond, including its wide band gap, optical transparency, and mechanical strength.[3−6] Although carbon nanofilaments have also been studied as novel carbon materials that can be used for catalysis,[7] no carbon material made of sp^3 carbon atoms (diamond) has been examined as a catalyst support material.

These observations led us to use oxidized diamond in a novel way. Oxidized diamond-supported metal oxide or metal catalysts exhibit excellent catalytic activity for the dehydrogenation of ethane,[8] synthesis gas formation from methane,[9] and decomposition of methanol.[10] In these reactions, weak but significant interactions between metals or metal oxides and the oxidized diamond surface on which they are loaded seem to play important roles in enhancing and prolonging the activity of the respective catalysts. The oxidized diamond acts as a solid carbon oxide material and provides an excellent support material for catalysts.

Recently, fuel cells have been promoted as one route to the development of zero-emission motor vehicles. Hydrogen is a very attractive clean fuel for reducing atmospheric pollution. However, significant problems are involved in the economic production and use of large quantities of hydrogen fuel without coproducing CO_2. If hydrogen could be produced efficiently, it could be a clean universal fuel. Methane is an attractive source of

---

* To whom correspondence should be addressed. Tel: +81-29-851-3354, ext. 8259. Fax: +81-29-851-4005. E-mail: c-diamond@md.neweb.ne.jp.

[†] National Institute for Materials Science (NIMS).

[‡] Kansai University.

[§] National Institute of Advanced Industrial Science and Technology (AIST).

[||] University of Tsukuba.

[⊥] Core Research for Evolutional Science and Technology (CREST) of Japan Science and Technology Corporation (JST) and NIMS.

(1) Inagaki, M. *New Carbons − Control of Structure and Functions*; Elsevier Scientific Publications: Amsterdam/New York, 2000; pp 1−240.

(2) Buriak, J. M. *Angew. Chem., Int. Ed.* **2001**, *40*, 532.

(3) Ando, T.; Inoue, S.; Ishii, M.; Kamo, M.; Sato, Y.; Yamada, O.; Nakano, T. *J. Chem. Soc., Faraday Trans.* **1993**, *89*, 749.

(4) Ando, T.; Ishii, M.; Kamo, M.; Sato, Y. *J. Chem. Soc., Faraday Trans.* **1993**, *89*, 1383.

(5) Ando, T.; Ishii, M.; Kamo, M.; Sato, Y. *J. Chem. Soc., Faraday Trans.* **1993**, *89*, 1783.

(6) Ando, T.; Yamamoto, K.; Ishii, M.; Kamo, M.; Sato, Y. *J. Chem. Soc., Faraday Trans.* **1993**, *89*, 3635.

(7) Mestl, G.; Maksimova, N. I.; Keller, N.; Roddatis, V. V.; Schlögl, R. *Angew. Chem., Int. Ed.* **2001**, *40*, 2066.

(8) Nakagawa, K.; Kajita, C.; Ikenaga, N.; Kobayashi, T.; Gamo, M. N.; Ando, T.; Suzuki, T. *Chem. Lett.* **2000**, 1100.

(9) Nakagawa, K.; Nishimoto, H.; Enoki, Y.; Egashira, S.; Ikenaga, N.; Kobayashi, T.; Gamo, M. N.; Ando, T.; Suzuki, T. *Chem. Lett.* **2001**, 460.

(10) Nakagawa, K.; Hashida, T.; Kajita, C.; Ikenaga, N.; Kobayashi, T.; Gamo, M. N.; Suzuki, T.; Ando, T. *Catal. Lett.* **2002**, *80*, 161.

10.1021/cm0210997 CCC: $25.00

hydrogen. Decomposition of methane is an effective hydrogen production process, and can feed a fuel cell (eq 1).

$$CH_4 \rightleftarrows 2H_2 + C \quad (1)$$

A hydrogen production process that does not involve CO is required, because CO strongly poisons the electrode of a fuel cell. Decomposition of methane has attracted a great deal of attention because the process requires little control of side reactions and yields reduced CO_2 emission.[11−13]

For the catalytic decomposition of methane to hydrogen to show a high catalytic activity and long lifetime, it is essential to form whisker- or fiber-type carbon and to keep active species isolated from the catalyst surface (eq 2).

$$CH_4 \rightleftarrows 2H_2 + C_{\text{whisker, fiber, tube}} \quad (2)$$

The nanometer-sized carbon fiber and tube that are formed together with hydrogen are very interesting and unique carbon materials. In contrast, catalytic sites are covered and deactivation occurs when (as in eq 3) the carbon is formed as soot, amorphous or encapsulated carbon on the catalyst surface, and catalytic activity for the decomposition of methane is then very low.[14,15]

$$CH_4 \rightleftarrows 2H_2 + C_{\text{soot, amorphous, encapsulated}} \quad (3)$$

In this paper, we focus on oxidized diamond, which interacts weakly with loaded active metal species. We will deal with the decomposition of methane over oxidized diamond-supported metal catalysts. We have found that Ni- and Pd-loaded oxidized diamond catalysts markedly promote the decomposition of methane and simultaneously produce novel carbon composite materials made of a combination of diamond (sp^3 carbon) and nanocarbon materials (sp^2 carbon).

Experimental Section

Preparation of Catalyst. The preparation of oxidized diamond has been described previously.[8] Catalysts were prepared by impregnating an aqueous solution of metal nitrates or chlorides onto oxidized diamond (surface area (SA) 12.6 m^2/g), activated carbon (Wako pure chemical, SA 948 m^2/g), Al_2O_3 (JRC-ALO-4, the reference catalyst provided by the Catalyst Society of Japan, SA 161 m^2/g), SiO_2 (Wako pure chemical, SA 194 m^2/g), TiO_2 (Japan Aerosil Co. SA 47.0 m^2/g), MgO (Ube Industries, Ltd., SA 144 m^2/g), ZrO_2 (SA 40.0 m^2/g), Y_2O_3 (SA 12.9 m^2/g), La_2O_3 (SA 23.7 m^2/g), and CeO_2 (SA 50.7 m^2/g). The catalytic supports of ZrO_2, Y_2O_3, La_2O_3, and CeO_2 were prepared by thermal decomposition of $ZrO_2 \cdot nH_2O$, $Y_2(C_2O_4) \cdot 4H_2O$, $La(CH_3COO)_3 \cdot {}^3/_2H_2O$, and $Ce(NO_3)_3 \cdot 6H_2O$ (Nacalai tesque, Inc.) at 873 K under air for 5 h. Oxidized diamond-supported group VIII metal catalysts containing 3 or 5 wt % of group VIII metal were prepared by impregnating an aqueous solution of $Fe(NO_3)_3 \cdot 9H_2O$, $Co(NO_3)_2 \cdot 6H_2O$, $Ni(NO_3)_2 \cdot 6H_2O$ (Wako pure chemical), $RuCl_3 \cdot nH_2O$, $RhCl_3 \cdot H_2O$, $Pd(CH_3COO)_2$, $IrCl_4 \cdot H_2O$, and $(NH_3)_2Pt(NO_2)_2$ (Mitsuwa Pure Chemicals) into the suspended support materials, followed by evaporation to dryness. Supported catalysts were dried and calcined at 723 K for 5 h in air prior to use. Prior to the reaction, the catalyst was reduced with H_2 at 673 K for 1 h.

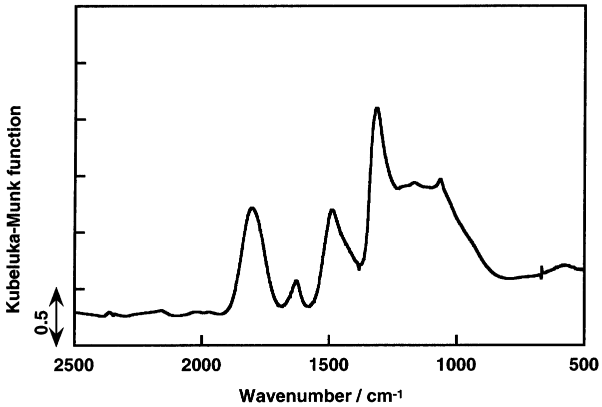

Figure 1. Diffuse reflectance FT-IR spectra of oxidized diamond.

Catalytic Reaction. The decomposition of methane was carried out in a thermogravimetric analyzer (TGA-50, Shimadzu) at atmospheric pressure. Using 13 mg of a catalyst, 15 mL/min of CH_4 and 15 mL/min of Ar were introduced at 873 K. Gaseous products were analyzed by a Shimadzu GC8AIT (TCD detector) gas chromatograph.

Characterization. Surface area of the catalyst was measured by the BET method using N_2 at 77 K and an automatic Micromeritics Gemini model 2375. Scanning electron microscopy (SEM) results were observed using a Hitachi S-4500. Transmission electron microscope (TEM) results were obtained using a JEOL JEM-2010 (200 kV) on catalyst samples so that the morphology of the deposited carbon could be determined.

Results and Discussion

Diffuse Reflectance FT-IR Spectroscopic Analysis of Oxidized Diamond. Figure 1 shows the diffuse reflectance FT-IR spectrum of oxidized diamond. Scheme 1 is the proposed model of oxidized diamond. The spectrum of oxidized diamond contained bands in the region of 1650−1850 cm^{-1}, which were ascribed to C=O stretching vibrations (νC=O), and absorptions at 1150 and 1250 cm^{-1} were assigned to C−O−C stretching vibrations (νC−O). These results indicate that oxygen species were introduced onto the diamond surface.

Effect of Support on the Catalytic Activity of Ni-Loaded Catalysts. Figure 2 shows the catalytic activity for the decomposition of methane over various Ni (5 wt %)-loaded metal oxide catalysts observed by TG traces. Catalytic decomposition of methane was carried out at 873 K. Each trace shows the weight increase of the catalyst, and these weight increases have indicated the consumption of methane to give carbon materials and yielding H_2. H_2 was the only gaseous product obtained from the decomposition of methane over Ni-loaded catalysts. The order of catalytic activity using different support materials at a reaction temperature of 873 K was as follows: oxidized diamond > SiO_2 > CeO_2 > ZrO_2 > TiO_2, La_2O_3 > Al_2O_3 > Y_2O_3 > MgO. These results indicate that the catalytic activity for decomposition of methane over the Ni-loaded catalysts depended strongly upon the support material. Among Ni-loaded catalysts, only the diamond-supported catalyst afforded a high conversion of methane, and a

---

(11) Ishihara, T.; Miyashita, Y.; Iseda, H.; Takita, Y. *Chem. Lett.* **1995**, 93.

(12) Otsuka, K.; Seino, T.; Kobayashi, S.; Takenaka, S. *Chem. Lett.* **1999**, 1179.

(13) Wang, P.; Tanabe, E.; Ito, K.; Jia, J.; Morioka, H.; Shishido, T.; Takehira, K. *Appl. Catal. A.* **2002**, *231*, 35.

(14) Nakagawa, K.; Ikenaga, N.; Teng, Y.; Kobayashi, T.; Suzuki, T. *J. Catal.* **1999**, *186*, 405.

(15) Rostrup-Nielsen, J. R. In *Catalysis, Science and Technology*; Anderson J. R., Boudart, M., Eds.; Springer: Berlin, 1984; Vol. 5, pp 1−117.

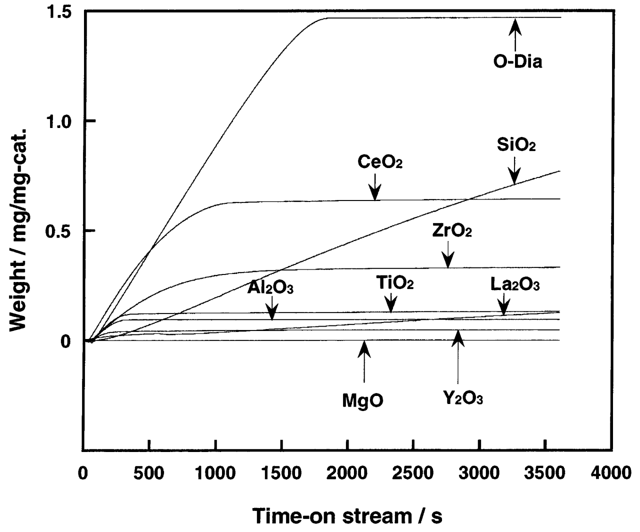

Figure 2. Carbon deposition from CH_4 on Ni-loaded catalysts at 873 K. Reaction conditions: flow rate, 30.0 mL/min (CH_4/Ar = 1); metal loading level, 5 wt %. Prior to reaction, catalysts were reduced with H_2 at 873 K for 1 h.

Table 1. Comparative Characteristics of Ni-Loaded[a] Catalysts

catalyst	H_2 reduction temperature (K)	specific surface area (m^2/g)	average size of Ni particles (nm)
Ni/oxidized diamond	873	12	4.9
Ni/SiO_2	873	180	12

[a] Ni loading level = 5 wt%.

significant H_2 yield. The high activity of Ni-loaded oxidized diamond catalyst is noteworthy, considering that the surface area of oxidized diamond is quite small. It is well-known that Ni-loaded catalysts exhibit a high catalytic activity for decomposition of methane. Among the supports, Ni loaded on a SiO_2 catalyst is reported to be the one of the most active catalysts.[11−13] Although the oxidized diamond (12.6 m^2/g) had a smaller specific surface area than that of SiO_2 (194 m^2/g), oxidized diamond exhibited higher activity than SiO_2. The average sizes of Ni particles on oxidized diamond and SiO_2 are shown in Table 1. The average particle sizes of Ni on oxidized diamond and SiO_2 measured by XRD peak widths were about 4.9 and 12 nm, respectively. The catalytic activity of the oxidized diamond-supported Ni catalyst did not depend on the specific surface area of the support material. Generally, the catalytic activity of a metal-loaded catalyst is affected by the particle size of the loaded metal. If the particle size is smaller, the activity is expected to increase. A larger specific surface area of a support material is expected to yield a higher dispersion of the loaded metal particles, i.e., the metal particle size will decrease on surfaces with larger specific surface areas. Because of the larger surface area of SiO_2, the particle size of Ni should be smaller than that on the oxidized diamond. The smaller size of the Ni on SiO_2 was expected to show higher activity than that of the oxidized diamond. However, the activity of the oxidized diamond-supported Ni catalyst was higher than that of SiO_2-supported Ni catalyst. The particle size of Ni on the diamond was smaller than that on SiO_2. The particle size of Ni on the diamond was not related to the smaller surface area of oxidized diamond.

Oxygen species on the support material surface played an important role in the control of redox properties of active metal species on the support materials. Although both activated carbon and graphite are composed only of carbon, it is interesting that the activated carbon and graphite-supported Ni catalysts exhibited negligible catalytic activities for the decomposition of methane under the reaction conditions employed here. Among carbon materials, only the oxidized diamond-supported catalyst showed a significant catalytic activity. The results were similar to those in the synthesis gas production from methane[9] and the decomposition of methanol.[10] The reason for the differences in the catalytic activities of oxidized diamond and activated carbon or graphite is unclear. Though oxidized diamond has C−O−C ether-type structures and C═O carbonyl-type structures on its surface,[3−6] few functional groups exist on graphite, and on active carbon surfaces no ether or carbonyl functional groups were seen. The oxygen

Scheme 1. Proposed Model of Oxidized Diamond

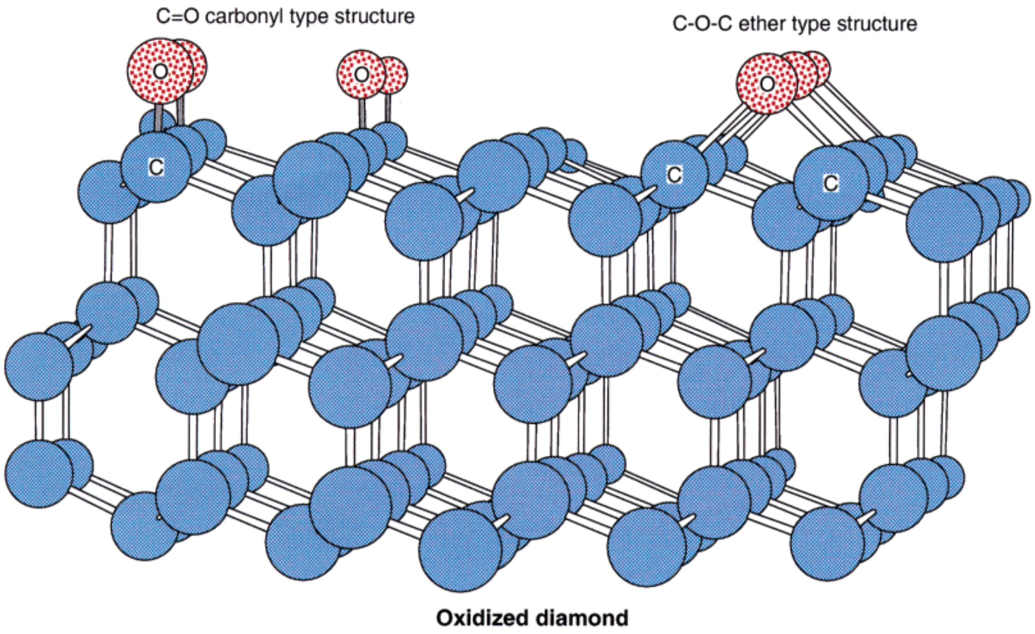

Table 2. Effect of Temperature of Ni (5 wt%)/Oxidized Diamond Catalyst on the Decomposition of Methane[a]

temperature (K)	conversion CH_4 (%)	yield H_2 (mmol)	yield carbon (mmol)
723	4.9	2.6	1.3
773	7.1	3.8	1.9
823	14.9	8.0	4.0
873	21.3	11.4	5.7

[a] Catalyst, 0.06 g; flow rate of CH_4, 10.0 mL/min (26.8 mmol/h); reaction time = 1 h; space velocity = 10000 h^{-1} mL g-cat^{-1}.

species on the surface of the support material might play an important role in controlling the catalytic performance of the loaded metal species.

To produce hydrogen with a high yield, metallic Ni is required.[16] If Ni species are highly dispersed on strong or moderately basic metal oxide surfaces such as MgO, Y_2O_3, and La_2O_3, the Ni oxide might be stabilized and only with difficulty be reduced to metallic Ni. Even in this case, there was some reduction to hydrogen.[16] In contrast, in the case of Ni species dispersed on the strong or moderately acidic metal oxides, Ni species would be stabilized as metallic Ni. Rapid carbon deposition would occur on the catalyst surface and active sites might be covered by amorphous or encapsulated carbon (eq 3).[15] Supported-metal catalysts are known to show unique properties such as strong metal–support interaction (SMSI).[17,18] Ma et al. have reported that the nature of support materials could play an important role in the morphological characteristics and the chemical state of loaded metal in the carbonaceous medium-supported Cu catalysts.[19] In the case of the oxidized diamond-supported system, the surface oxygen species might maintain the loaded Ni in the active state. Such a synergistic promotion effect on the active phase is believed to be the reason for the observed support effect. We consider that the high level of activity of the oxidized diamond-supported catalyst originated from the chemical interaction between the loaded Ni and the oxidized diamond support surface.

Table 2 shows the effect of temperature on the H_2 and carbon yield over the oxidized diamond-supported Ni (5 wt %) catalyst. H_2 and carbon yields increased with increasing reaction temperature, and the highest H_2 and carbon yields were obtained at 873 K.

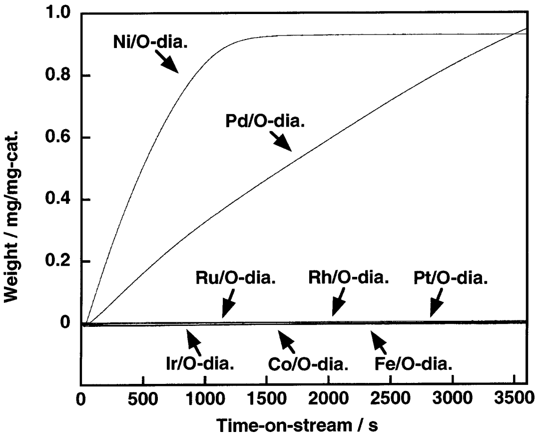

Figure 3. Carbon deposition from methane on various oxidized diamond-supported metal catalysts at 873 K. Reaction conditions: flow rate, 30.0 mL/min (CH_4/Ar = 1); metal loading level, 3 wt %. Prior to reaction, catalysts were reduced with H_2 at 873 K for 1 h.

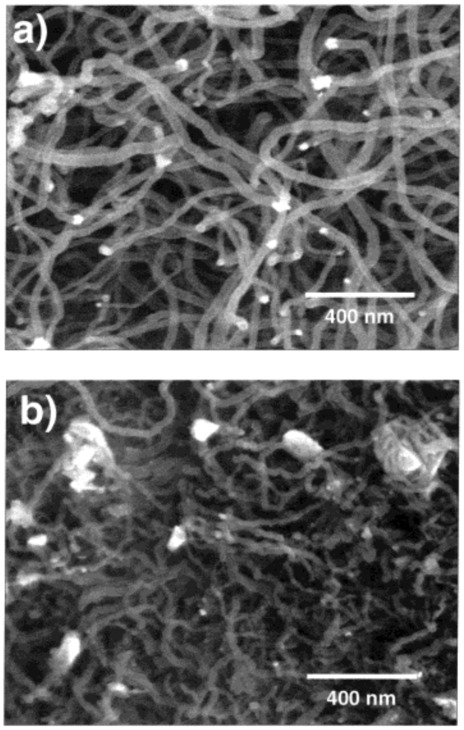

Figure 4. SEM images of carbon nanomaterials obtained by decomposition of methane over (a) Ni/oxidized diamond, and (b) Pd/oxidized diamond.

Group VIII Metals on the Catalytic Decomposition of Methane. Figure 3 shows the catalytic activity for the decomposition of methane by oxidized diamond-supported metal (3 wt %) catalysts. Prior to the reaction, all catalysts were reduced with H_2 at 873 K for 1 h. At 873 K, the order of catalytic activity of metal species was as follows: Ni > Pd ≫ Fe, Co, Ru, Rh, Ir, Pt. Among the oxidized diamond-supported metal catalysts, only oxidized diamond-supported Ni and Pd catalysts afforded a high conversion of methane and a significant H_2 yield. Whisker carbon was confirmed with Ni- and Pd-loaded oxidized diamond catalysts (eq 2). The oxidized diamond-supported Pd catalyst produced a high rate of methane conversion. Pd/TiO_2 catalyst has been reported to promote the decomposition of methane.[20] Oxidized diamond-supported Pd catalyst also afforded high catalytic activity. In contrast, Rh-containing catalysts are well-known to be one of the most highly active catalysts for this reaction.[14,20] However, the oxidized diamond-supported Rh catalyst did not exhibit catalytic activity under the reaction conditions employed.

Characterization of Carbon Nanomaterials. Figure 4 a and b show scanning electron microscope (SEM) images of carbon nanomaterials on oxidized diamond-supported Ni and Pd catalysts, respectively. The carbon nanomaterials were prepared by the decomposition of

---

(16) Nakagawa, K.; Ikenaga, N.; Suzuki, T.; Teng, Y.; Kobayashi, T. *Appl. Catal. A* **1999**, *180*, 183.

(17) Geus, J. W. In *Chemisorption and Reactions on Metallic Films*; Academic Press: New York, 1971; Vol. 1, p 129.

(18) Tauster, S. J.; Fung, S. C.; Baker, R. T. K.; Horsley, J. A. *Science* **1981**, *211*, 1121.

(19) Ma, J.; Rodriguez, N. M.; Vannice, M. A.; Baker, R. T. K. *J. Catal.* **1999**, *183*, 32.

(20) Nakagawa, K.; Ikenaga, N.; Kobayashi, T.; Suzuki, T. *Catal. Today* **2001**, *64*, 31.

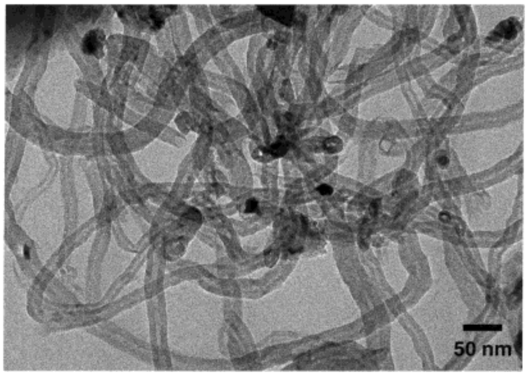

Figure 5. TEM images of carbon nanomaterials obtained by decomposition of methane over Ni/Oxidized diamond catalyst.

methane at 873 K over oxidized diamond-supported Ni and Pd catalysts, and although their diameters and lengths differ, both show zigzag structures. Although it is premature to discuss the role of metal particles or species, these observations suggest that the formation mechanisms and characteristics of the carbon nanomaterials formed over oxidized diamond-supported Ni and Pd strongly depend on the loaded metal species. Figure 5 shows transmission electron microscope (TEM) images of carbon nanomaterials on oxidized diamond-supported Ni catalyst. As seen in the TEM image, the major carbon nanomaterial over the oxidized diamond-supported Ni catalyst has a coaxial hollow channel. Various methods of synthesizing tubular carbon filaments or carbon nanotubes have been reported, including the disproportionation of CO,[21−23] the thermal decomposition of hydrocarbons,[24−26] arc discharge,[27,28] laser ablation,[29] plasma CVD,[30] and liquid-phase nanoamorhozo.[31,32] In-depth studies of the catalytic formation of filamentous carbon have been reported by Baker et al.[33,34] Mechanisms of carbon nanofilament formation using metal-loaded catalysts have been proposed.[35−37] As regards the mechanism, Baker et al. have reported that the first stage involves the decomposition of a hydrocarbon (acetylene) on the front surface of a metal particle (Ni), producing H_2 and carbon. The dissolved carbon then diffuses through the particle, to be deposited on the trailing face, forming the carbon filament.[33] However, the mechanism of carbon nanofilament formation using Ni-loaded oxidized diamond catalyst is still not clear.

Conclusions

In summary, among Ni-loaded catalysts, oxidized diamond support showed the highest catalytic activity for the decomposition of methane to produce hydrogen for a fuel cell. Oxidized diamond was useful as a novel unique catalytic support material. When oxidized diamond was used as a catalyst support material, Ni-loaded oxidized diamond catalyst showed the highest H_2 yield. Whisker-type carbon nanomaterials were produced on Ni- and Pd-loaded oxidized diamond catalysts by the decomposition of methane. We suggest that the high level of activity of the oxidized diamond-supported catalyst was the result of chemical interaction between the loaded metal such as Ni or Pd and the oxidized diamond support surface. The present findings also suggest that the surface properties of oxidized diamond have the potential to produce unique catalytic reactions, such as hydrogen production from methane.

Acknowledgment. This work was financially supported by Grant-in Aid for Scientific Research (B) 14350429 from the Japan Society for the Promotion of Science (JSPS). K. Nakagawa is grateful for his fellowship for Young Scientists from JSPS.

CM0210997

---

(21) Davis, W. R.; Slawson, R. J.; Rigby, G. R. *Nature* **1953**, *171*, 756.

(22) Hofer, L. J. E.; Sterling, E.; McCartney, J. T. *J. Phys. Chem.* **1955**, *59*, 1153.

(23) Audier, M.; Oberlin, A.; Coulon, M. *J. Cryst. Growth* **1982**, *57*, 524.

(24) Tibbetts, G. G. *J. Cryst. Growth* **1984**, *66*, 632.

(25) Oberlin, A.; Endo, M.; Koyama, T. *J. Cryst. Growth* **1976**, *32*, 335.

(26) Sacco, A., Jr.; Geurts, F. W. A. H.; Jablonski, G. A.; Lee, S.; Gately, R. A. *J. Catal.* **1989**, *119*, 322.

(27) Bacon, R. *J. Appl. Phys.* **1960**, *31*, 283.

(28) Iijima, S. *Nature* **1991**, *354*, 56.

(29) Thess, A.; Lee, R.; Nikolaev, P.; Dai, H.; Petit, P.; Robert, J.; Xu, C.; Lee, Y. H.; Kim, S. G.; Rinzler, A. G.; Colbert, D. T.; Scuseria, G. E.; Tomanek, D.; Fischer, J. E.; Smally, R. E. *Science* **1996**, *273*, 483.

(30) Ren, Z. F.; Huang, Z. P.; Xu, J. W.; Wang, J. H.; Bush, P.; Siegal, M. P.; Provencio, P. N. *Science* **1998**, *282*, 1105.

(31) Zhang, Y.; Gamo, M. N.; Xiao, C.; Ando, T. *Jpn. J. Appl. Phys.* **2002**, *41*, L408.

(32) Zhang, Y.; Gamo, M. N.; Nakagawa, K.; Ando, T. *J. Mater. Res.* **2002**, *17*, 2457.

(33) Baker, R. T. K.; Barber, M. A.; Harris, P. S.; Feates, F. S.; Waite, R. J. *J. Catal.* **1972**, *26*, 51.

(34) Baker, R. T. K.; Harris, P. S.; Thomas, R. B.; Waite, R. J. *J. Catal.* **1973**, *30*, 86.

(35) Baker, R. T. K.; Harris, P. S. In *Chemistry and Physics of Carbon;* Walker, P. L., Jr., Thrower, P. A., Eds.; Marcel Dekker: New York, 1978; Vol. 14, p 83.

(36) Rodriguez, N. M. *J. Mater. Res.* **1993**, *8*, 3233.

(37) Baker, R. T. K. *J. Adhesion* **1995**, *52*, 13.